

# Inductively Compensated Parallel Coupled Microstrip Lines and Their Applications

Ravee Phromlousri, Mitchai Chongcheawchamnan, *Member, IEEE*, and Ian D. Robertson, *Senior Member, IEEE*

**Abstract**—A simple method using lumped inductors to compensate unequal even- and odd-mode phase velocities in parallel coupled microstrip lines is presented. The singly and doubly compensated cases are analyzed to enable the optimum inductor values and the electrical lengths of the compensated coupled lines to be calculated from closed-form expressions. The technique proposed not only improves the performance, but also yields a more compact design. To demonstrate the technique's broad range of applicability, the compensated coupled-line structure is used to enhance the performance of a 900-MHz Lange coupler, a 1-GHz multisection 10-dB coupler, a 900-MHz planar Marchand balun, and a 1.8-GHz parallel coupled bandpass filter.

**Index Terms**—Coupled-line resonator, Marchand balun, microstrip, parallel coupled filter, parallel coupled lines.

## I. INTRODUCTION

**P**ARALLEL-COUPLED lines are extensively used in microwave and millimeter-wave circuits for filters, impedance-matching networks, directional couplers, baluns, and combiners [1], [2]. Since microstrip is easily incorporated in hybrid and monolithic microwave integrated circuits [3], it is the most common technology for microwave and millimeter-wave circuits. As microstrip is an inhomogeneous medium, parallel coupled microstrip lines exhibit poor directivity [4] resulting from the inequality of even- and odd-mode wave phase velocities [5], [6].

The unequal phase velocities in parallel coupled microstrip lines not only cause poor directivity in couplers, but also significantly deteriorate the performance of other circuit components circuits. For example, it is well known that the parallel coupled microstrip bandpass filter has an asymmetrical passband response and spurious responses at harmonics of the filter passband [7]. It was recently reported [8] that degradation in amplitude/phase balance of the microstrip Marchand balun partly stems from the unequal phase velocities. Over the past decades, the notorious problem of unequal phase velocities in parallel coupled microstrip lines has been tackled by several previously proposed techniques. The techniques can be classified into two main categories, which are distributed and lumped compensation approaches.

The methodology based on the distributed approach is to modify either the parallel coupled-line structure [9], [10], dielectric layer [11], or ground plane [12] such that the phase velocities of both modes are equalized. No external components or extra space are needed for this approach. The main disadvantage of this approach is the lack of closed-form design equations, meaning the design task heavily relies on the electromagnetic (EM) simulation stage, which, in turn, consumes much effort and computing time. Additionally, techniques based on this approach are often not suitable for some standard fabrication processes, thus more cost demand is unavoidably required.

The lumped compensation approach [1], [13], [14] involves connecting external reactive components between or shunted with the parallel coupled-lines' ports. Based on the reactive types, this approach can be categorized into two techniques, which are capacitive [1], [13], [14] and inductive compensation techniques [13]. The size of the lumped-compensated parallel coupled lines is about the same as the original size (the uncompensated coupled lines) since the length of compensated parallel coupled lines is shorter than that of the uncompensated coupled lines. Another distinct advantage of the lumped compensation technique is its simple design procedure because the closed-form design equations can be derived. The disadvantages of the technique are, from a practical point-of-view, the lumped components' parasitics and difficulty in layout [1], [13]. In this paper, we present a simple, yet effective inductive compensation technique to improve the directivity of the parallel coupled microstrip lines. The technique can achieve high isolation and, hence, high-directivity coupled microstrip lines by connecting small inductors in series with the coupled-lines' ports.

This paper is organized as follows. Section II presents two proposed inductive compensation techniques, referred to as the singly and doubly compensated cases. Analysis of the techniques will be performed and closed-form equations for determining the optimum values of inductor for the singly and doubly compensated cases are provided. The derived closed-form equations are validated by comparison with analysis results of the uncompensated and compensated coupled lines. Applications of the inductively compensated coupled-line structure to a Lange coupler, a three-section 10-dB coupler, a planar Marchand balun, and a parallel coupled microstrip bandpass filter will be demonstrated in Section III. The design equations for these circuits are also given. Design examples of the circuits based on the inductively compensated coupled-line section as well as the EM simulated and measured results will be presented in Section IV. This paper is then concluded in Section V.

Manuscript received December 27, 2005; revised April 26, 2006.

R. Phromlousri and M. Chongcheawchamnan are with the Research Center of Electromagnetic-Wave Applications and Telecommunication Department, Mahanakorn University of Technology, Bangkok, Thailand.

I. D. Robertson is with the School of Electronic and Electrical Engineering, The University of Leeds, Leeds LS2 9JT, U.K.

Color versions of Figs. 10, 13, 16, and 20 are available online at <http://ieeexplore.ieee.org>.

Digital Object Identifier 10.1109/TMTT.2006.881026

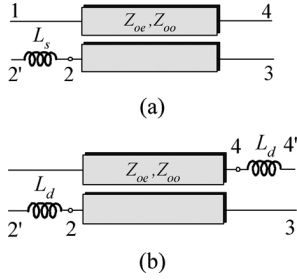


Fig. 1. Schematics of: (a) singly and (b) doubly compensated parallel coupled lines.

## II. INDUCTIVELY COMPENSATED COUPLED LINES

Due to the different phase velocities associated with the even- and odd-mode wave propagation, parallel coupled microstrip lines cannot easily achieve directivity values better than 12 dB [3]. Here, we propose an inductive compensation technique to equalize phase velocities in coupled microstrip lines, which, in turn, leads to a high isolation and, hence, high-directivity coupled microstrip lines. Both a singly and doubly compensated technique can be used.

### A. Singly Compensated Case

Fig. 1(a) shows the schematic of parallel coupled lines using a single inductor for compensation. The parallel coupled-line section has the characteristic impedance of  $Z_0$  and coupling coefficient of  $k$ . Both  $k$  and  $Z_0$  are related to the even- and odd-mode characteristic impedances ( $Z_{oe}$  and  $Z_{oo}$ ) of the parallel coupled lines [3]. The compensated inductor ( $L_s$ ) is connected in series with the coupled port (port 2), giving what we define as port 2', the coupled port of the compensated coupled-line section. As the compensated inductor ( $L_s$ ) is connected in series with the coupled port of the uncompensated parallel coupled lines, open-circuited impedance parameters ( $Z$ -parameter) are more appropriate to analyze this problem.

Assuming the uncompensated coupled lines are symmetrical, the  $Z$ -parameters of the coupled lines can be characterized completely by just four elements of the uncompensated parallel coupled lines'  $Z$ -parameter matrix denoted by  $z_{11}$ ,  $Z_{12}$ ,  $Z_{13}$ , and  $Z_{14}$ . Applying the two-port network theory to the circuit of Fig. 1(a) [15], the  $Z$ -parameters of the singly compensated parallel coupled lines ( $\mathbf{Z}_s$ ) in matrix form can be written as

$$\mathbf{Z}_s(f) = \begin{bmatrix} Z_{11} & Z_{12} & Z_{13} & Z_{14} \\ Z_{12} & Z_{11} + j2\pi f L_s & Z_{14} & Z_{13} \\ Z_{13} & Z_{14} & Z_{11} & Z_{12} \\ Z_{14} & Z_{13} & Z_{12} & Z_{11} \end{bmatrix}. \quad (1)$$

Terminating the singly compensated coupled lines shown in Fig. 1(a) with  $Z_0$  at all ports and then applying the  $S$ -parameter definitions, the coupling ( $S'_{12}$ ) and isolation coefficients ( $S_{13}$ ) of the singly compensated coupled lines can be obtained from

$$S_{12'} = 2V_1/V_{g2'} \quad (2a)$$

$$S_{13} = 2V_1/V_{g3}. \quad (2b)$$

From (2a),  $S_{12'}$  is the ratio between the voltage at port 1 ( $V_1$ ) and the voltage source injected at coupled port (port 2'), which

is denoted by  $V_{g2'}$ . Similarly,  $S_{13}$  from (2b) is the ratio between the terminal voltage at port 1 ( $V_1$ ) and the voltage source injected at the isolated port (port 3), which is denoted by  $V_{g3}$ . The directivity of the singly compensated coupled-line section is immediately obtained by dividing  $S_{12'}$  from (2a) by  $S_{13}$  from (2b). The compensating inductor  $L_s$  can improve  $S_{13}$  considerably with a small change in  $S_{12'}$ . Thus, the optimum value of  $L_s$  with such a condition can be solved. For our analysis, we apply the  $Z$ -parameters obtained from (1) into (2) to solve for the optimum value of  $L_s$ . At the operating frequency of  $f_0$ , this  $L_s$  must provide the minimum magnitude of  $S_{13}$  and minimum difference between  $S_{12'}$  and  $k$ , the original coupling coefficient. After some mathematical manipulation, we obtain the optimum value of  $L_s$  shown as follows [16]:

$$L_s = \frac{Z_0}{4\pi f_0} \operatorname{Im} \left\{ \frac{-Z_0 \partial + j(Z_{oe} \sin \theta_e - Z_{oo} \sin \theta_o)}{Z_0 \partial + j(Z_{oe} \sin \theta_o - Z_{oo} \sin \theta_e)} \right\} \quad (3a)$$

where  $\operatorname{Im}\{Z\}$  denotes an imaginary part of  $Z$  and

$$\partial = \cos \theta_o - \cos \theta_e \quad \Theta = \sqrt{\frac{\varepsilon_{\text{effo}}}{\varepsilon_{\text{effe}}}}$$

where: 1)  $\varepsilon_{\text{effe}}$  is the even-mode effective dielectric constant; 2)  $\varepsilon_{\text{effo}}$  is the odd-mode effective dielectric constant; 3)  $\theta_e = (\pi/2)$  is the even-mode electrical length of the uncompensated coupled lines; and 4)  $\theta_o = (\pi/2)\Theta$  is the odd-mode electrical length of the uncompensated coupled lines.

Note that the frequency where maximum directivity is obtained for the singly compensated technique does shift slightly below the original  $f_0$ . Therefore, the electrical length of the singly compensated coupled lines ( $\theta_s$ ) must be modified as follows [16]:

$$\theta_s(L_s) = \frac{1}{\Theta} \cot^{-1} \left( \frac{2\pi f_0 L_s}{Z_{oo}} \right). \quad (3b)$$

### B. Doubly Compensated Case

The doubly compensated technique applied to parallel coupled microstrip lines is shown in Fig. 1(b). Here, two identical compensating inductors ( $L_d$ ) are connected in series with the coupled (port 2) and direct ports (port 4) of the uncompensated parallel coupled microstrip lines. We assume that the uncompensated coupled-line section shown in Fig. 1(b) is symmetrical and the impedance parameters are  $Z_{11}$ ,  $Z_{12}$ ,  $Z_{13}$ , and  $Z_{14}$ . The coupled and direct ports of the compensated coupled lines are now port 2' and 4', respectively.

The analysis procedure for this structure is similar to the procedure applied to a singly inductive compensation case, which was already described in Section II-A. From Fig. 1(b), the  $Z$ -parameters of the doubly inductive-compensated coupled lines ( $\mathbf{Z}_d$ ) in matrix form can be written as

$$\mathbf{Z}_d(f) = \begin{bmatrix} Z_{11} & Z_{12} & Z_{13} & Z_{14} \\ Z_{12} & Z_{11} + j2\pi f L_d & Z_{14} & Z_{13} \\ Z_{13} & Z_{14} & Z_{11} & Z_{12} \\ Z_{14} & Z_{13} & Z_{12} & Z_{11} + j2\pi f L_d \end{bmatrix}. \quad (4)$$

With similar conditions and similar approach applied in Section II-A, the optimum value of  $L_d$  connecting in series at ports 2' and 4' can be determined as follows [16]:

$$L_d = \frac{Z_0}{2\pi f_0} \text{Im} \left\{ \frac{Z_0(\cos \theta_o - \cos \theta_e) + Z_B - \Re}{Z_B} \right\} \quad (5)$$

where

$$\Re = j\sqrt{(Z_{oo}^2 + Z_{oe}^2) \sin \theta_e \sin \theta_o + 2Z_0^2(\cos \theta_e \cos \theta_o - 1)} \quad (6a)$$

and

$$Z_B = j(Z_{oe} \sin \theta_o - Z_{oo} \sin \theta_e). \quad (6b)$$

Again,  $f_0$  slightly shifts from the original  $f_0$ . Hence, to shift  $f_0$  where maximum directivity occurs back to the original, the electrical length of the doubly compensated coupled lines ( $\theta_d$ ) must be shortened as follows [16]:

$$\theta_d(L_d) = \frac{1}{\Theta} \cot^{-1} \left[ \frac{2\pi f_0 L_d}{Z_{oo}} - \frac{1}{2} \cot \left( \frac{\pi}{2} \Theta \right) \right]. \quad (7)$$

### C. Analysis Results and Performances

The validity of the inductive compensation technique is proven by applying the technique to a microstrip 10-dB coupler operating at 1.8 GHz  $f_0$ . The substrate used is RF60–0600 from Taconic Inc., Petersburg, NY ( $\epsilon_r = 6.45$ ,  $h = 1.52$  mm, and  $\tan \delta = 0.002$ ). Based on these parameters,  $L_s$  and  $L_d$  calculated from (3a) and (5) are 1.24 and 1.31 nH, respectively. In all cases,  $Z_{oe}$  is 69.37  $\Omega$  and  $Z_{oo}$  is 36.03  $\Omega$ . The degree of directivity and isolation improvement of the inductive compensation technique is compared with two capacitive compensation techniques [1], [4]. The compensated capacitors are 0.185 [1] and 0.187 pF [4].

Simulations of all of these coupled-line topologies are performed and the results compared. We assume that the inductive and capacitive lumped components used are ideal. Fig. 2(a) shows the simulation results of directivity and isolation performances of the capacitive compensation techniques [1], [4] in comparison with the uncompensated 10-dB parallel coupled microstrip lines. From 1.5 to 2.1 GHz, the directivity performances of both techniques are at least 12 [1] and 14 [4] dB more than that of the uncompensated design. Fig. 2(b) shows the simulation of directivity and isolation performance of singly and doubly compensated cases. The directivity and isolation performances from the singly and doubly compensated techniques are 6 and 11 dB better, respectively, than those of the uncompensated coupled lines from 0.7 to 2.7 GHz. At the  $f_0$  of 1.8 GHz, the doubly compensated design provides isolation and directivity performance approximately 25 dB better than the uncompensated coupled lines, while the singly compensated design achieves around 8-dB improvement.

Comparing the performances between inductive and capacitive compensation techniques, we find that the doubly compensated technique provides best directivity improvement for a narrowband design. Although the performance of the capacitive compensation techniques is better for wideband design, such relatively small capacitors needed in the design examples may

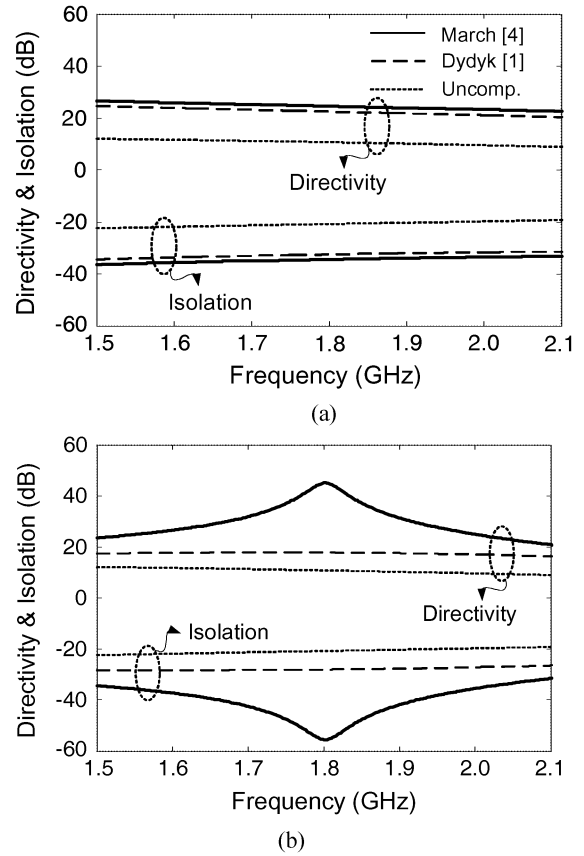


Fig. 2. Simulation results of directivity and isolation performances of the: (a) previous works and (b) singly (---) and doubly (—) compensated 10-dB coupled lines compared with the uncompensated case (···).

cause practical limitations for some applications. In addition, layout of the capacitive compensation technique is more difficult than the proposed technique. For the RF60–0600 substrate, gains of the capacitive-compensated [1], [4] and the proposed compensated coupled microstrip lines' directivities over the uncompensated coupled-lines' directivities at  $f_0$  for each coupling factor are shown in Fig. 3 (top). At least 7.5- and 10-dB directivity gain is achieved from the singly and doubly compensated cases over the coupling factor range of  $-1$  to  $-15$  dB. From  $-3$  to  $-11$ -dB coupling factor, the doubly inductive and capacitive compensation techniques exhibit a similar degree of directivity gain. For very tight coupling, only the singly compensated case provides the directivity gain.

The effect of deviation in optimum compensated components on the directivity (described in terms of percentage of directivity variation) of both inductively and capacitively compensated coupled lines has also been studied. Fig. 3 (bottom) shows the analysis results of the percentage of directivity variation when optimum inductors or capacitors are deviated within  $\pm 10\%$ . The directivity sensitivity of the singly compensated case is constant around 20% from over  $-1$ - to  $-15$ -dB coupling factor. It is shown in Fig. 3 that the directivity of the doubly compensated technique is not very sensitive to  $L_d$ , especially for tight coupling. Maximum sensitivity result from the effect of component variation is owned by the capacitive-compensated design proposed in [4]. However, it should be noted that

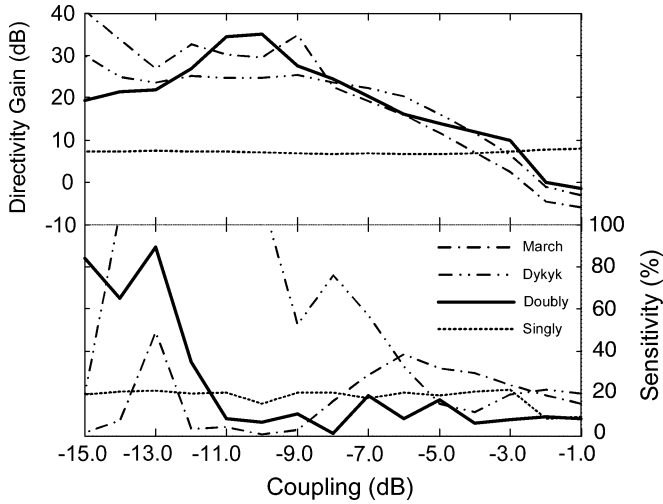


Fig. 3. (top) Directivity gain over the uncompensated design at  $f_0$  and (bottom) its variation over 10% change of optimum compensated inductors on the RF60-0600 substrate.

such deviations are solely specified to parallel coupled lines designed on the specific substrate, not for any substrate and not necessarily coupled-line-based circuits. The effect of deviation in compensating inductor values on the performance of other coupled-line based circuits should be carefully considered for each design case.

### III. APPLICATION CIRCUITS

In order to demonstrate the usefulness of the inductive compensation technique, it is applied to four frequently used parallel coupled microstrip circuits: the Lange coupler, a three-section coupler, the planar Marchand balun and, finally, the parallel coupled bandpass filter.

#### A. Lange Coupler

The Lange coupler is a popular tight quadrature coupler used in microwave circuit design. It has been well known that the tight coupling in the Lange coupler is achieved by increasing the odd-mode capacitance with the numbers of parallel line because the parallel-line structure in a Lange coupler causes poor directivity, especially at the high-frequency band edge when realizing a Lange coupler in microstrip technology. To solve this problem, either the singly or doubly compensated technique can be applied to the Lange coupler. For the sake of brevity, here we demonstrate only the design detail of the singly compensated Lange coupler. For the doubly compensated Lange coupler, the design procedure is similar. Fig. 4 shows the singly compensated technique applied to a Lange coupler. The odd- and even-mode characteristic impedances are  $Z_{oo}$  and  $Z_{oe}$ , respectively. The compensated inductor  $L_s$  is connected at the coupled port and the electrical length is  $\theta_s$ . With these parameters, the singly compensated Lange coupler can be fully characterized by (1). Consequently,  $L_s$  and  $\theta_s$ , shown in Fig. 4, are calculated from (3a) and (3b) for designing the singly compensated Lange coupler.

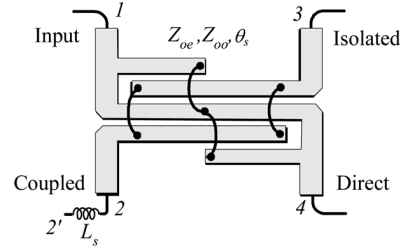


Fig. 4. Singly compensated Lange coupler.

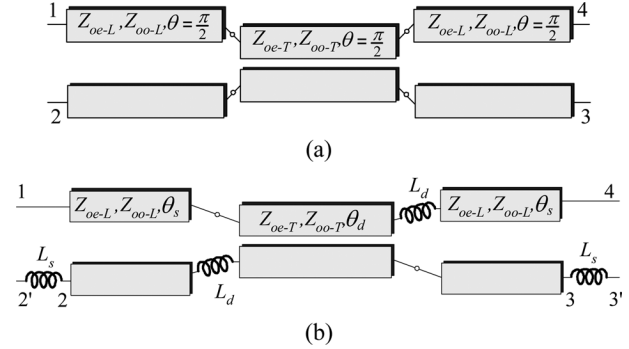


Fig. 5. Schematics of: (a) uncompensated and (b) inductive-compensated three-section coupled lines.

#### B. Multisection Parallel Coupled Lines

Parallel coupled lines with multioctave bandwidth can be realized using a multisection topology. However, the poor directivity of each parallel coupled-line section deteriorates the isolation performance and degrades the coupling bandwidth. The proposed inductive compensation technique applied to each parallel coupled-line section preserves the desired coupling bandwidth, as well as improves the isolation performance of the multisection parallel coupled lines. Since there are various parallel coupled lines in the multisection topology, numerous forms of inductive-compensation-based multisection parallel coupled lines can be obtained by applying each coupled-line section with different combinations of singly and/or doubly compensated techniques. In this paper, we apply a combination of singly and doubly compensated designs to a three-section 10-dB coupler.

Fig. 5(a) and (b) shows the schematics of the uncompensated and inductively compensated three-section coupled lines, respectively. As shown in Fig. 5(b), the singly and doubly compensated techniques are applied to the outer and center coupled lines, respectively. The design procedure of the compensated multisection coupled lines follows that of the uncompensated coupled lines [17], [18]. After obtaining the parameters of each parallel coupled-line section, all the uncompensated parallel coupled lines will be replaced with the inductive-compensated parallel coupled lines. The compensated inductors  $L_s$  and  $L_d$  are calculated from (3a) and (5). The electrical lengths of each coupled-line section ( $\theta_s, \theta_d$ ) are calculated from (3b) and (7). Finally, based on these electrical parameters, the physical parameters of each coupled-line section are synthesized.

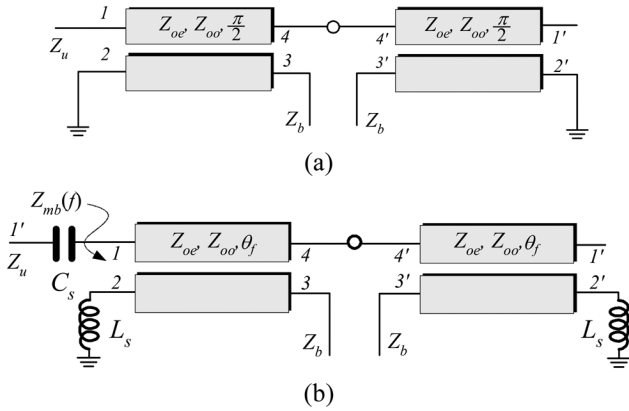


Fig. 6. Schematics of: (a) uncompensated and (b) singly compensated coupled-line-based Marchand balun.

### C. Marchand Balun

Having been extensively used in a large variety of microwave circuits, the planar Marchand balun is basically formed by two parallel coupled-line sections connected in back-to-back configuration, as shown in Fig. 6(a). The coupled-line section has coupling coefficient of  $k$ , characteristic impedance of  $Z_0$ , and electrical length of  $\pi/2$ . This conventional (uncompensated) Marchand balun can transform unbalanced port impedance ( $Z_u$ ) to balanced port impedance ( $Z_b$ ) if one selects  $k$  as follows [8]:

$$k = \frac{1}{\sqrt{\frac{2Z_b}{Z_u} + 1}}. \quad (8)$$

It has been reported that the Marchand balun exhibits poor amplitude/phase balance when the circuit is realized in inhomogeneous medium such as microstrip. The imbalance partly comes from the poor directivity of the parallel coupled microstrip lines [8], hence, an approach to improve the directivity of the coupled lines can enhance the amplitude/phase balance of the Marchand balun. For simplicity's sake, the singly compensated technique is applied to the Marchand balun. Fig. 6(b) shows the proposed technique based on the singly compensated technique. The optimum value of  $L_s$  can be calculated from (3a). From Fig. 6(b), the driving-point impedance at unbalanced port (port 1) at  $f_0$ , denoted by  $Z_{mb}(f_0)$ , is calculated from the  $Z$ -parameter of the singly compensated coupled line.

As is already known, each  $Z$ -parameter of the compensated coupled-line section can be obtained from (1). This  $Z$ -parameter will be used as basis parameter to calculate  $Z_{mb}(f_0)$ . For our analysis, the electrical length of each compensated coupled-line section ( $\theta_f$ ) is obtained by applying the following condition:

$$\text{Re}[Z_{mb}(f_0)] \approx Z_u. \quad (9)$$

Hence,

$$\theta_f(L_s) = \frac{1}{2\Theta Z_{oo}} \left[ 4\pi f_0 L_s + Z_{oo} \cot\left(\frac{\pi}{2}\Theta\right) \right]. \quad (10)$$

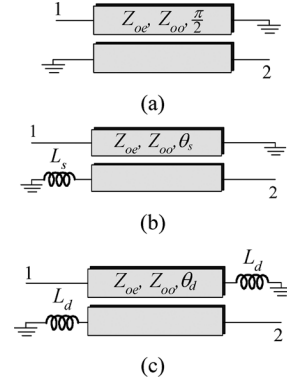


Fig. 7. Schematic of: (a) uncompensated, (b) singly, and (c) doubly compensated coupled-line resonators.

Designing the proposed balun with  $L_s$  and  $\theta_f$  calculated from (3) and (10), the real part of  $Z_{mb}(f_0)$  is nearly equal to  $Z_u$ , while the imaginary part of  $Z_{mb}(f_0)$  is inductive. This inductive part must be cancelled out to give the compensated Marchand balun good matching at the unbalanced port. The inductive part can be simply eliminated by a series capacitor ( $C_s$ ). The value of  $C_s$  can be determined by

$$C_s = \frac{1}{2\pi f_0 \text{Im}\{Z_{mb}(f_0)\}}. \quad (11)$$

It should be noted that  $C_s$  has little effect on the amplitude/phase balance of the balun. It significantly affects to only the return loss at the unbalanced port. The design procedure of the balun based on the singly compensated coupled lines starts by determining  $k$  from (8). With the known substrate and uncompensated coupled-line parameters, all electrical parameters ( $Z_{oo}$ ,  $Z_{oe}$ ,  $\theta_o$ ,  $\theta_e$ ,  $\epsilon_{\text{eff}e}$ , and  $\epsilon_{\text{eff}o}$ ) can be calculated. Subsequently,  $L_s$  is calculated from (3a). Finally,  $\theta_f$  and  $C_s$  are obtained from (10) and (11), respectively. With this design procedure, a balun design with good amplitude/phase balance and good return loss at the unbalanced port across a large bandwidth can be obtained.

### D. Parallel Coupled Filter

In an inhomogeneous medium such as microstrip, each coupled-line resonator in the parallel coupled filter cooperatively contributes a spurious response at twice the center frequency ( $2f_0$ ) and beyond. Since the poor directivity is an outcome of phase-velocity inequality, the inductively compensated coupled-line resonator with high directivity can suppress the spurious response of the filter effectively [19]. The resonators based on uncompensated and compensated coupled lines, both singly and doubly compensated cases, are depicted in Fig. 7(a)–(c), respectively. The optimum values of compensating inductors  $L_s$  and  $L_d$  in Fig. 7(b) and (c) can be determined from (3a) and (5).

To preserve the original filter response, the transmission response ( $S_{21}$ ) of the compensated resonator would be preserved or minimally change from that of the uncompensated resonator. Hence, this condition will be applied for extracting the electrical lengths of each compensated coupler. For tight coupling

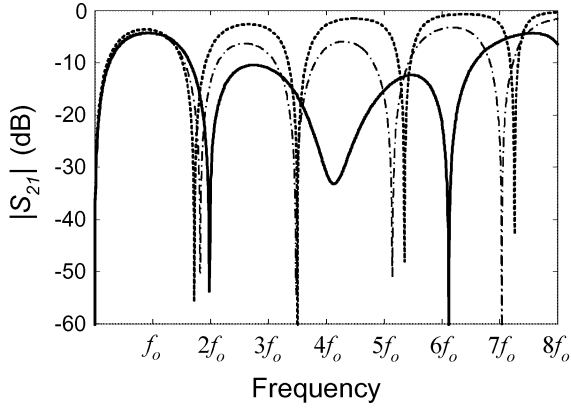


Fig. 8. Analysis results of frequency responses of the singly (---) and doubly (—) compensated coupled-line resonators compared with the uncompensated case (---).

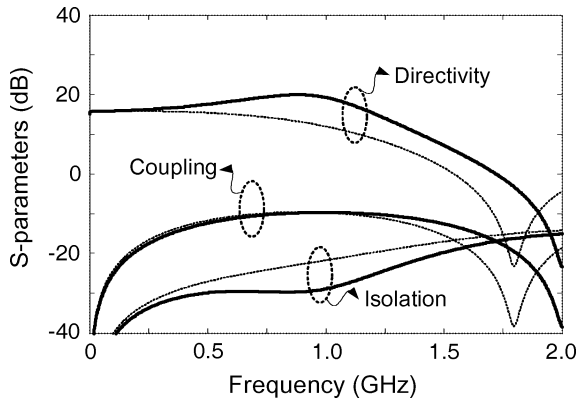


Fig. 9. Simulated frequency responses of the uncompensated (---) and singly compensated (—) Lange couplers.

( $k > -13$  dB), the electrical length of the singly inductive-compensated coupled-line resonator ( $\theta_s$ ) can be determined by

$$\theta_s(L_s) = \cot^{-1} \left( \frac{4\pi f_0 L_s - Z_{oo} \cot \left( \frac{\pi}{2} \Theta \right)}{2Z_{oe}} \right) \quad (12a)$$

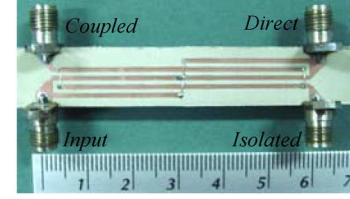
and for loose coupling ( $-23$  dB  $< k < -13$  dB),

$$\theta_s(L_s) = \frac{1}{\Theta} \cot^{-1} \left( \frac{4\pi f_0 L_s - Z_{oe} + Z_{oo} \cot \left( \frac{\pi}{2} \Theta \right)}{2Z_{oo}} \right). \quad (12b)$$

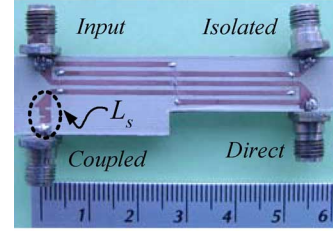
For the doubly compensated coupled-line resonator, its electrical length ( $\theta_d$ ) can be calculated from

$$\theta_d(L_d) = \cot^{-1} \left( \frac{Z_{oo} \cot \left( \frac{\pi}{2} \Theta \right) + 4\pi f_0 L_d}{2Z_{oe}} \right). \quad (13)$$

To explicitly show the spurious-suppression performances of both singly and doubly compensated coupled-line resonators, two resonators based on the proposed techniques were designed, and their frequency responses are compared with the results of the uncompensated parallel coupled resonator. We start with the



(a)



(b)

Fig. 10. PCB photographs of: (a) conventional and (b) singly compensated Lange couplers.

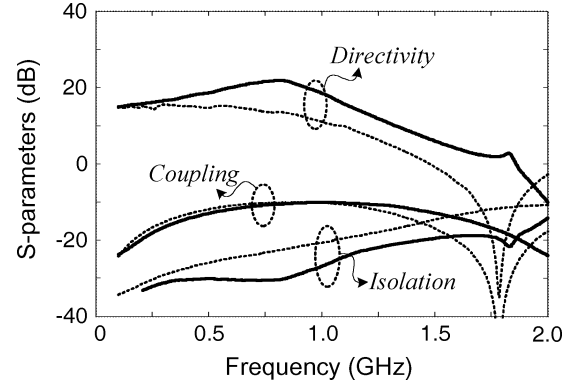


Fig. 11. Measured results of the singly (—) compensated and uncompensated (---) Lange couplers.

uncompensated coupled-line resonator. The resonator was designed from 8.6-dB parallel coupled lines operating at 1.0 GHz on an RF60–0600 microwave substrate from Taconic Inc.

The required value of  $Z_{oe}$  is found to be 78.84  $\Omega$  and  $Z_{oo}$  is 36.48  $\Omega$ . The values of  $L_s$ ,  $L_d$ ,  $\theta_s$ , and  $\theta_d$  for singly and doubly compensated coupled-line resonators were calculated from (3a), (5), (12), and (13). The values of  $L_s$ ,  $L_d$ ,  $\theta_s$ , and  $\theta_d$  are found to be 2.13 nH, 2.07 nH,  $0.46\pi$ , and  $0.44\pi$ , respectively. With these parameters, the frequency responses of three resonators are plotted in Fig. 8. As shown in Fig. 8, the magnitude of  $S_{21}$  of the uncompensated coupled-line resonator (shown as the dotted line) is around  $-7$  dB at the first harmonic of the desired passband response ( $2f_0$ ). Comparing the responses obtained from the singly and doubly compensated resonators with that obtained from the uncompensated resonator, the magnitudes of  $S_{21}$  around  $f_0$  are nearly equal, while the responses around  $2f_0$  and beyond are distinctly different. The suppression performances obtained from the compensated coupled-line resonators at odd and even harmonics of  $f_0$  are considerably better than the uncompensated coupled-line resonator. For the singly compensated case, the degree of suppression at  $2f_0$ ,  $3f_0$ , and  $4f_0$  are approximately 14, 7, and 7 dB, respectively, while the

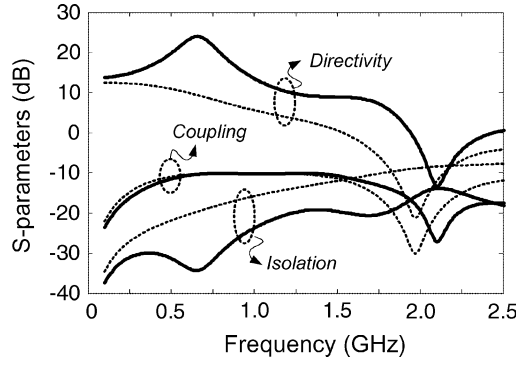


Fig. 12. Simulated frequency responses of the uncompensated (---) and compensated (—) three-section couplers.

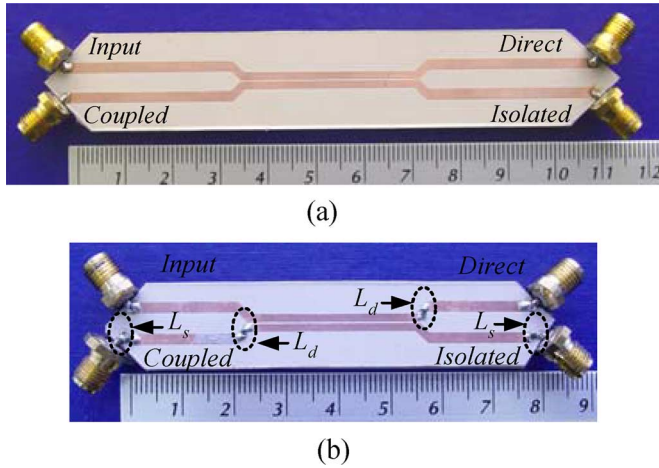


Fig. 13. PCB photographs of: (a) uncompensated and (b) compensated three-section couplers.

doubly compensated case gives 50, 15, and 30 dB, respectively. To apply the compensated coupled-line resonators to bandpass filter design, the uncompensated coupled-line resonators are initially synthesized. Each coupled-line resonator is then replaced with the singly or doubly compensated coupled-line resonator. All electrical parameters of the compensated coupled-line resonators are calculated from (3a), (5), (12), and (13) according to the singly or doubly compensation case. Finally, the dimensions of each proposed resonator are synthesized from the derived electrical parameters. Noted that the doubly inductive compensated technique proposed can be applied to suppress considerable spurious response for narrowband design due to the technique itself being narrowband.

#### IV. DESIGN AND EXPERIMENTAL RESULTS

##### A. Lange Coupler

An example of the singly compensated Lange coupler is demonstrated with a 10-dB coupler operating at 0.9 GHz on an RF35–0600 microwave substrate from Taconic Inc. ( $\epsilon_r = 3.5, h = 1.52$  mm,  $\tan \delta = 0.002$ ). It is noted that such a coupling factor is chosen for implementation sake due to the tolerance limitation of our in-house fabrication process. The required  $Z_{oe}, Z_{oo}$  values of the singly compensated design are  $69.37 \Omega$  and  $36.03 \Omega$ .  $L_s$  and  $\theta_s$  calculated from (3a) and (3b) are 2.05 nH and  $0.44\pi$ , respectively. The simulated results

TABLE I  
PARAMETERS OF THE THREE-SECTION COUPLERS @ 1.0 GHz

	$\theta_s, \theta_d$	$L_s, L_d$ (nH)	W,S,L (Loose) (mm)	W,S,L (Tight) (mm)
Uncomp.	$0.50\pi, 0.50\pi$	-	2.1, 4.35	1.6, 0.2, 36
Inductive	$0.31\pi, 0.43\pi$	3.9, 2.7	2.1, 4.22	1.6, 0.2, 32

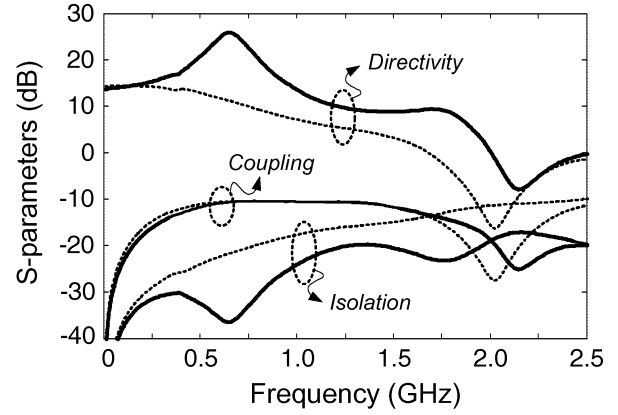


Fig. 14. Measured results of the: (a) uncompensated (---) and (b) compensated (—) three-section coupler.

TABLE II  
PARAMETERS OF THE BALUNS @ 0.9 GHz

Balun	$Z_{oe}$ ( $\Omega$ )	$Z_{oo}$ ( $\Omega$ )	$C_s$ (pF)	$L_s$ (nH)	$\theta_r$
Uncompensated	74.42	33.59	-	-	$0.5\pi$
Singly inductive	74.42	33.59	11.5	1.95	$0.42\pi$

of the coupling, isolation, and directivity performances of the uncompensated and singly compensated 10-dB Lange couplers are shown in Fig. 9.

The printed circuit board (PCB) photographs of the uncompensated and singly compensated Lange coupler are shown in Fig. 10(a) and (b), respectively. The sizes are  $10 \times 60$  mm<sup>2</sup> and  $10 \times 55$  mm<sup>2</sup>. The measurement was performed with an HP8720C vector network analyzer test system. Fig. 11 shows the measured isolation, coupling, and directivity performances of the singly compensated and uncompensated Lange couplers.

The measured results are in good agreement with the simulated results shown in Fig. 9. The directivity of the singly compensated one is improved by around 8 dB at 0.9 GHz compared to the uncompensated one. Moreover, the singly compensated Lange coupler provides directivity that is 6 dB better than that of the uncompensated Lange coupler across a 500-MHz bandwidth.

##### B. Three-Section Parallel Coupled Lines

Next, a three-section 10-dB maximally flat coupler operating at 1.0 GHz on an RF60–0600 substrate was designed and simulated for a 50- $\Omega$  system. Followed from the procedure of the conventional design [17], [18],  $-27.2$  and  $-8.2$ -dB coupled-line sections are needed for the outer and center sections shown in Fig. 5(b). From these required coupling coefficients, we obtain  $Z_{oe-L} = 52.23 \Omega$ ,  $Z_{oo-L} = 47.86 \Omega$ ,  $Z_{oe-T} = 75.55 \Omega$ , and  $Z_{oo-T} = 33.05 \Omega$ . These uncompensated parallel coupled

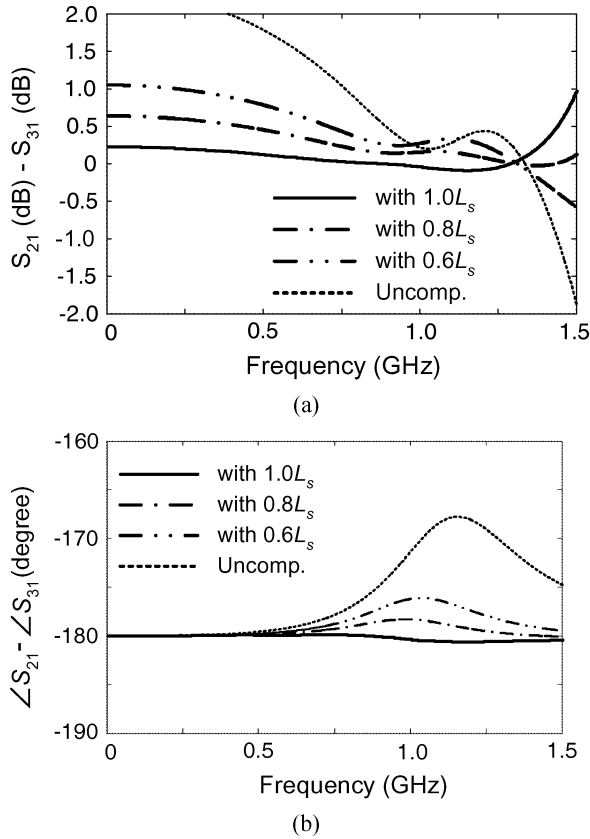


Fig. 15. Analysis results of: (a) amplitude and (b) phase imbalance of the 50–150-Ω compensated Marchand balun with various values of the compensating inductors.

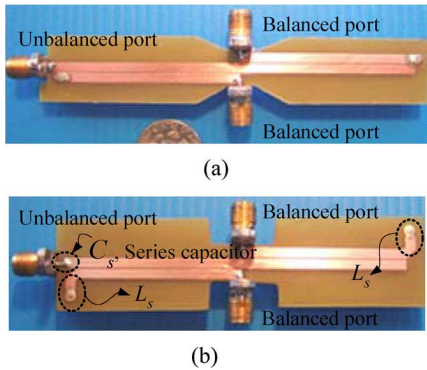


Fig. 16. PCB photographs of the fabricated: (a) uncompensated and (b) singly compensated Marchand balun.

lines are then converted to singly and doubly compensated coupled-line sections. The values of  $L_s$ ,  $L_d$ ,  $\theta_s$ , and  $\theta_d$  needed for these compensated coupled lines calculated from (3a), (5), (3b), and (7) are 4.14 nH, 1.88 nH,  $0.36\pi$ , and  $0.43\pi$ , respectively. The simulated results of the coupling, isolation, and directivity performances of the compensated and uncompensated three-section parallel coupled lines are shown in Fig. 12. The PCB photographs of the uncompensated and compensated three-section couplers are shown in Fig. 13(a), and (b), respectively. The electrical and physical parameters of the uncompensated and the compensated three-section parallel coupled lines are summarized in Table I. The size of the compensated three-section

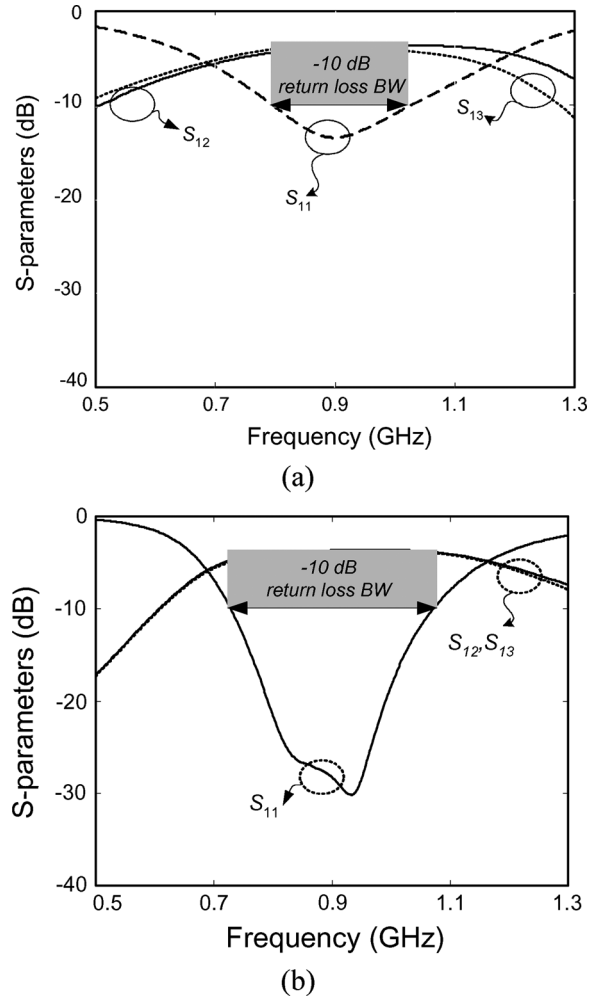


Fig. 17. Measured amplitude response of: (a) uncompensated and (b) singly compensated Marchand balun.

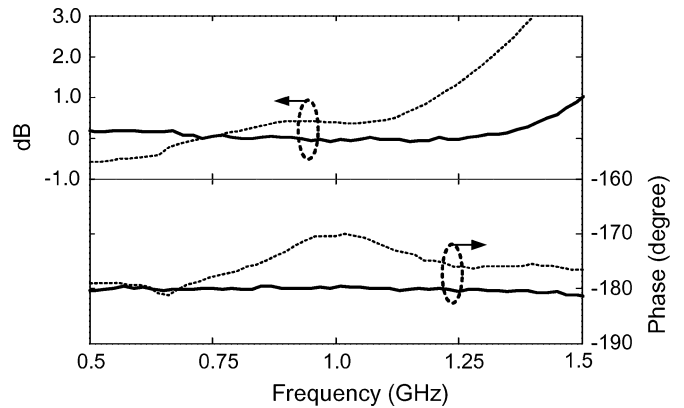


Fig. 18. Comparison of the measured (*upper*) magnitude and (*lower*) phase responses of the uncompensated (· · ·) and singly compensated (—) Marchand balun.

parallel coupled lines is  $10 \times 76 \text{ mm}^2$ , which is approximately 70% of the size of the uncompensated design ( $10 \times 107 \text{ mm}^2$ ).

The measured results of the proposed and the uncompensated three-section coupled lines are shown in Fig. 14. Clearly, the coupling bandwidth of the compensated coupler is better than that of the uncompensated coupler, which is degraded by poor



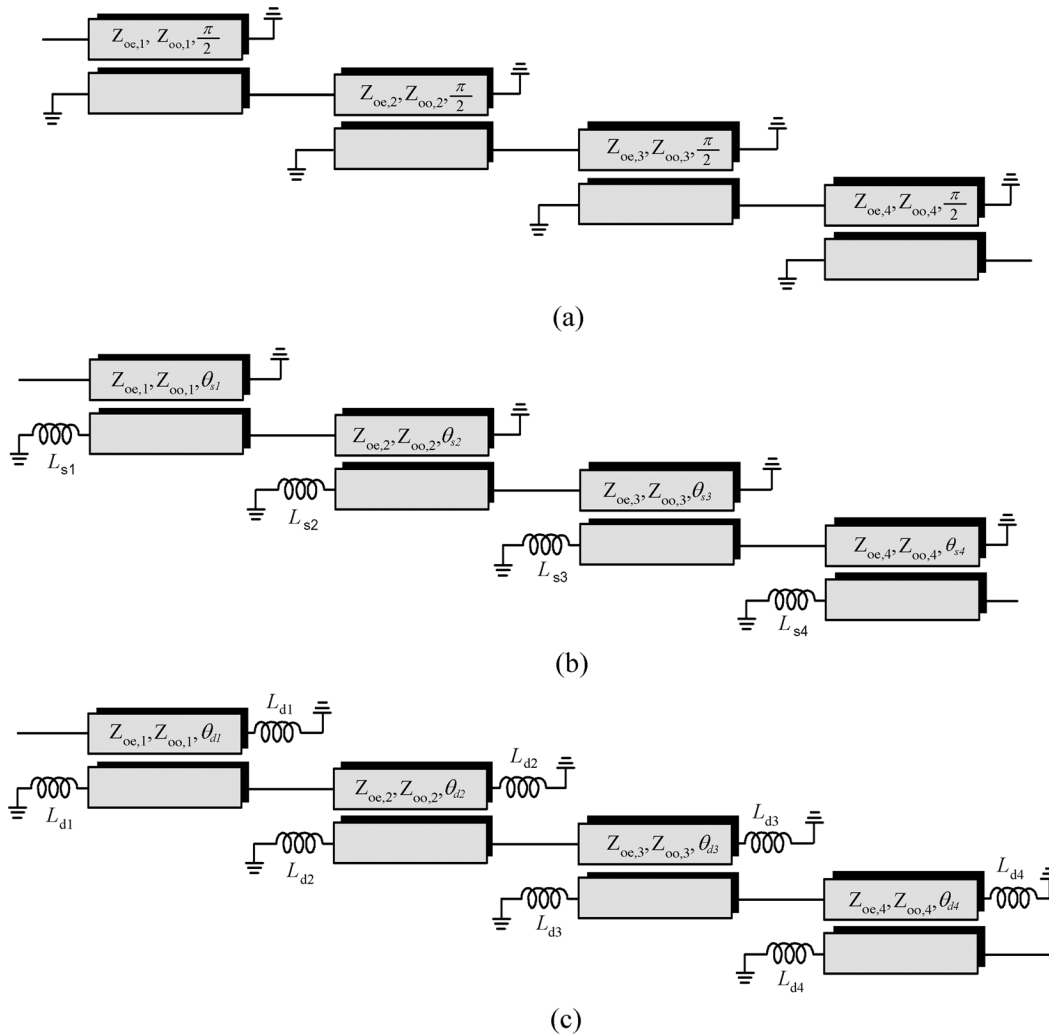


Fig. 19. Schematics of the third-order: (a) uncompensated, (b) singly, and (c) doubly compensated parallel coupled filters.

directivity in each uncompensated section. From the measured results, the directivity of the compensated coupler is 6.5 dB more than that of the uncompensated coupled lines over 80% of the operating bandwidth.

### C. Marchand Balun

To prove the validity of the technique for the Marchand balun, 900-MHz microstrip 50–150- $\Omega$  impedance transformation Marchand baluns based on the uncompensated and the singly compensated coupled lines were designed on an FR4 substrate ( $\epsilon_r = 4.55$ ,  $h = 1.6$  mm,  $\tan \delta = 0.02$ ). The  $Z_{oe}$  and  $Z_{oo}$  of the coupled lines are 74.42 and 33.59  $\Omega$ , respectively. The parameters calculated from (3a), (10), and (11) for these Marchand balun are shown in Table II.

The sensitivity to  $L_s$  of the amplitude/phase imbalance is investigated for the 50–150- $\Omega$  Marchand balun. Based on the analysis results, variations of amplitude and phase balance resulting from different compensated inductors are shown in Fig. 15(a) and (b), respectively. The amplitude and phase balance of the singly compensated Marchand balun is excellent across the operation bandwidth. The proposed technique is rather practical for the balun since the balance performance is not very sensitive

to the optimum value of the compensating inductor. As shown in Fig. 15(a) and (b), with the 20% change of compensating inductors, the amplitude imbalance of the balun is maintained within  $\pm 0.3$  dB and the phase difference is  $180^\circ \pm 2^\circ$  over a 30% bandwidth. The physical dimensions of the two baluns were synthesized from the parameters listed in Table II. Fig. 16(a) and (b) shows the PCB photographs of the designs. The measured frequency responses of the uncompensated Marchand balun are shown in Fig. 17(a).

The uncompensated Marchand balun achieved a 3.5-dB transmission coefficient and less than 13-dB return loss at the unbalanced port. The amplitude balance is good only at 900 MHz, while at other frequencies, especially in the high-frequency band edge, it is very poor. Fig. 17(b) shows the measured results of the singly compensated Marchand balun. At 900 MHz, the transmission coefficient is around 3.7 dB and the return loss of the unbalanced port is better than 25 dB. The proposed technique exhibits only 0.2 dB more loss than the uncompensated balun, which is due to loss from the series capacitor. Comparing the measured 10-dB return loss bandwidth, the bandwidth of the proposed technique is 170 MHz larger than the uncompensated balun.

TABLE III  
PARAMETERS OF THE FILTER DESIGNS

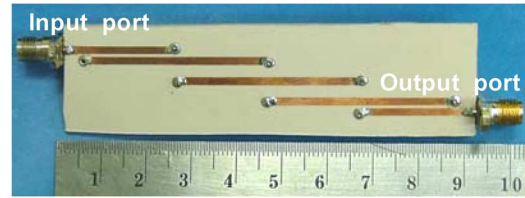
BPF	Section $i$	$Z_{oe,i}$ ( $\Omega$ )	$Z_{oo,i}$ ( $\Omega$ )	$L_{s,i}$ or $L_{d,i}$ (nH)	$\theta_{s,i}$ or $\theta_{d,i}$	W, S, L (mm)
Uncompensated	1,4	78.44	36.69	-	$0.50\pi$	1.45, 0.3, 20.1
	2,3	66.42	49.89	-	$0.50\pi$	1.55, 1.5, 19.6
Singly-compensated	1,4	78.44	36.69	1.7	$0.47\pi$	1.45, 0.3, 18.9
	2,3	66.42	49.89	2.5	$0.42\pi$	1.55, 1.5, 16.5
Doubly-compensated	1,4	78.44	36.69	1.2	$0.42\pi$	1.45, 0.3, 16.8
	2,3	66.42	49.89	2.5	$0.34\pi$	1.55, 1.5, 13.3

Fig. 18 shows the amplitude/phase balance of the uncompensated (shown as the dotted line) and the compensated Marchand balun (shown as the solid line). Compared with the uncompensated balun, the amplitude/phase balance of the singly compensated balun is considerably enhanced. The amplitude and phase balance of the proposed technique is excellent, with  $\pm 0.1$  dB and  $180^\circ \pm 1^\circ$  tracking from 700 MHz to 1.1 GHz.

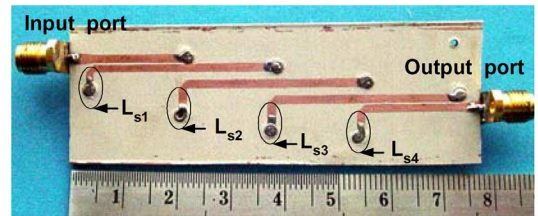
#### D. Parallel Coupled Filter

The effectiveness of the inductively compensated parallel coupled filter is proven with three filter designs. These three filters are an uncompensated, a singly, and a doubly compensated design. The filter prototype is a third-order Chebyshev bandpass filter designed at center frequency ( $f_0$ ) of 1.8 GHz, fractional bandwidth ( $\Delta$ ) of 10%, and passband ripple of 0.1 dB. The circuits were designed and fabricated on the RF60–0600 substrate from Taconic Inc. The schematics of three filters are depicted in Fig. 19(a)–(c), respectively. With the design procedure mentioned in Section III, the parameters of three filters were derived and are shown in Table III. The physical dimensions of all three filters are synthesized from the parameters in Section II. Fig. 20(a)–(c) shows the PCB photographs of three filters designed with the uncompensated, singly, and doubly compensated coupled-line section. In our design, the compensation inductors were implemented by shorted stubs. The total sizes of the singly and doubly compensated parallel coupled filters shown in Fig. 20(b) and (c) are  $17 \times 70$  mm<sup>2</sup> and  $18 \times 65$  mm<sup>2</sup>, which are approximately 85.4% and 84% of the uncompensated parallel coupled filter's size. Fig. 21 presents the EM simulated results of the uncompensated and the compensated parallel coupled filters.

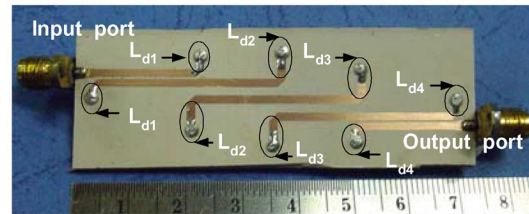
The frequency response of the uncompensated parallel coupled filter (dash line) evidently shows spurious response more than  $-12$  dB at  $2f_0$ . More than 45- and 28-dB suppression of the spurious response at  $2f_0$  and  $3f_0$  are obtained from the singly (dotted line) and doubly (thick line) compensated parallel coupled filters. The measurement was performed with an HP8720C vector network analyzer calibrated from 0.1 to 10 GHz. HPVVE6.0 software was used to collect the experimental data via a general-purpose interface bus (GPIB) card. Sonnet-Lite and MATLAB were used for simulation, data processing, and display. The measured results of the microstrip filter designed with the uncompensated and the singly compensated coupled-line resonators are shown in Fig. 22(a). The



(a)



(b)



(c)

Fig. 20. PCB photographs of: (a) conventional, (b) singly, and (c) the doubly compensated parallel coupled filters.

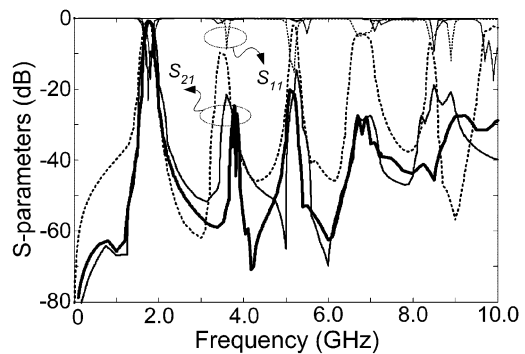


Fig. 21. Comparisons of EM simulated results of the singly (—) and doubly (—) compensated compared with the uncompensated case (---) parallel coupled filters.

measured insertion and both input/output return losses of the uncompensated filter are  $-1.2$  dB and better than  $-14$  dB, while the singly compensated filter's insertion and input/output

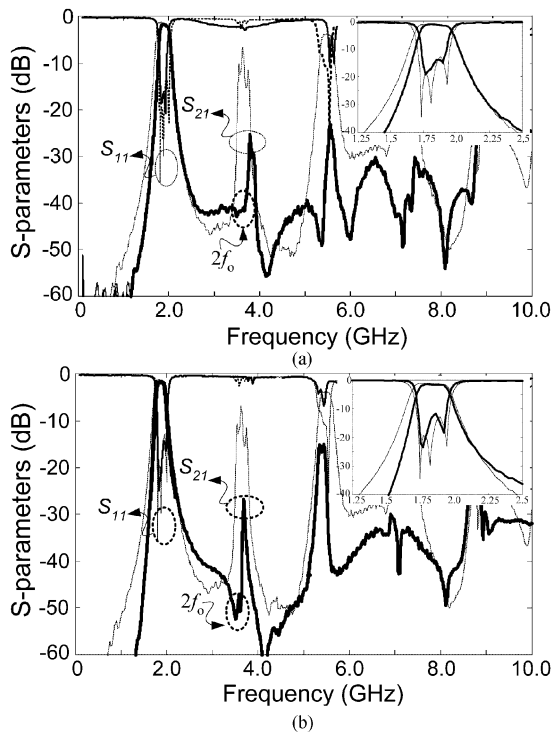


Fig. 22. Comparisons of measured results of: (a) singly (—) and (b) doubly (—) compensated compared with the uncompensated case (---) parallel coupled filters.

return losses are  $-1.4$  dB and better than  $-12$  dB, which is in good agreement with the EM simulated results.

The measured spurious response obtained from the uncompensated parallel coupled filter (dashed line) is around  $-13$  dB at  $2f_0$ . More than 39- and 42-dB suppression of spurious response at  $2f_0$  and  $3f_0$  are obtained from the singly compensated parallel coupled filter. Fig. 22(b) shows the measured results of the doubly compensated parallel coupled filter (thick line). The harmonic suppressions at  $2f_0$  and  $3f_0$  are more than 49 and 34 dB, respectively. Over the operating bandwidth, insertion losses are less than  $-1.5$  dB, while both input and output return losses are better than  $-12$  dB.

## V. CONCLUSIONS

Based on the simple inductive compensation technique proposed, we have presented two new methods to achieve high-directivity parallel coupled lines in microstrip. The compensating inductor connected in series with either coupled or direct port of the coupled-line structure equalizes phase velocity, leading to a high-directivity coupled-line design. Compared with previously proposed lumped compensation techniques, the inductive compensation technique provides better directivity performance for a 10% fractional bandwidth. The optimum value of compensation inductor is relatively small, so the technique can be implemented practically in microwave and millimeter-wave applications. The inductive compensation technique has been demonstrated in four microwave coupled-line-based microstrip circuits, which are the Lange coupler, multisection coupler, planar Marchand balun,

and parallel coupled bandpass filter. Design procedures for these circuits with the compensation technique have been described. The closed-form expressions for determining the compensation inductor values and coupled-line parameters simplify the design task. Since there are various microwave communication circuits whose structures consist of parallel coupled lines, it is believed that the technique is highly applicable and suitable for modern wireless communications.

## ACKNOWLEDGMENT

The authors are grateful to Taconic Inc., Petersburg, NY, for supplying the Taconic RF60-0600 microwave substrate for this research. The authors also thank the anonymous reviewers for their valuable comments and suggestions.

## REFERENCES

- [1] M. Dydyk, "Accurate design of microstrip directional couplers with capacitive compensation," in *IEEE MTT-S Int. Microw. Symp. Dig.*, May 1990, pp. 581–584.
- [2] G. L. Matthaei, L. Young, and E. M. T. Jones, *Microwave Impedance-Matching Network and Coupling Structures*. New York: McGraw-Hill, 1964, pp. 583–593.
- [3] T. Edward, *Foundation for Microstrip Circuit Design*. West Sussex, U.K.: Wiley, 1992, pp. 173–228.
- [4] S. L. March, "Phase velocity compensation in parallel-coupled microstrip," in *IEEE MTT-S Int. Microw. Symp. Dig.*, Jun. 1982, pp. 581–584.
- [5] A. Riddle, "High performance parallel coupled microstrip filter," in *IEEE MTT-S Int. Microw. Symp. Dig.*, May 1988, pp. 427–430.
- [6] S. M. Wang, C. H. Chen, and C. Y. Chang, "A study of meandered microstrip coupler with high directivity," in *IEEE MTT-S Int. Microw. Symp. Dig.*, Jun. 2003, pp. 63–66.
- [7] I. J. Bahl, "Capacitively compensated performance parallel coupled microstrip filter," in *IEEE MTT-S Int. Microw. Symp. Dig.*, Jun. 1989, pp. 679–682.
- [8] C. Y. Ng, M. Chongcheawchamnan, and I. D. Robertson, "Analysis and design of a high-performance planar Marchand balun," in *IEEE MTT-S Int. Microw. Symp. Dig.*, Jun. 2002, pp. 113–116.
- [9] A. Podell, "A high directivity microstrip coupled lines technique," in *IEEE MTT-S Int. Microw. Symp. Dig.*, May 1970, pp. 33–56.
- [10] S. Uysal and H. Aghvami, "Synthesis, design, and construction of ultra-wide-band nonuniform quadrature directional couplers in inhomogeneous media," *IEEE Trans. Microw. Theory Tech.*, vol. 37, no. 6, pp. 969–976, Jun. 1989.
- [11] C. S. Kim, Y. T. Kim, S. C. S. Kim, Y. T. Kim, S. H. Song, W. S. Jung, K. Y. Kang, J. S. Park, and D. Ahn, "A design of microstrip directional coupler for high directivity and tight coupling," *Eur. Gallium Arsenide and Other Semiconduct. Applicat. Symp.*, pp. 126–129, Sep. 2001.
- [12] F. R. Yang, Y. Qian, and T. Itoh, "A novel uniplanar compact structure for filter and mixer applications," *IEEE Trans. Microw. Theory Tech.*, vol. 47, no. 6, pp. 969–976, Jun. 1989.
- [13] M. Dydyk, "Microstrip directional couplers with ideal performance via single-element compensation," *IEEE Trans. Microw. Theory Tech.*, vol. 47, no. 6, pp. 956–964, Jun. 1999.
- [14] S. F. Chang, J. J. Chen, Y. H. Jeng, and C. T. Wu, "New high-directivity coupler design with coupled spurlines," *IEEE Microw. Wireless Compon. Lett.*, vol. 14, no. 2, pp. 65–67, Feb. 2004.
- [15] C. A. Desoer, *Basic Circuit Theory*. New York: McGraw-Hill, 1966, pp. 409–469.
- [16] R. Phromloungsri and M. Chongcheawchamnan, "A high directivity design using an inductive compensation technique," in *Asia-Pacific Microw. Conf.*, Dec. 2005, pp. 2840–2843.
- [17] E. H. Fook and R. A. Zakarevicius, *Microwave Engineering Using Microstrip Circuits*. New York: Prentice-Hall, 1990.
- [18] D. M. Pozar, *Microwave Engineering*, 2nd ed. New York: Wiley, 1998.
- [19] R. Phromloungsri, S. Patisang, K. Srisathit, and M. Chongcheawchamnan, "A harmonic-suppression microwave bandpass filter based on an inductively compensated microstrip coupler," in *Asia-Pacific Microw. Conf.*, Dec. 2005, pp. 2836–2839.



**Ravee Phromloungsri** was born in Khon Kaen, Thailand. He received the B.Sc. degree in applied physics in solid-state electronics from the King Mongkut Institute of Technology, Ladkrabang (KMITL), Thailand, in 1992, the M.Eng. degree in electrical engineering (telecommunication) from Mahanakorn University of Technology (MUT), Bangkok, Thailand, in 2000, and is currently working toward the D.Eng. degree in electrical engineering in MUT.

Since 1992, he has been a Lecturer with the Department of Telecommunication Engineering, MUT. He is a member of the Research Center of Electromagnetic Waves Applications (RCEWs). His research and teaching interests include microwave passive/active and RF circuits design.



**Mitchai Chongcheawchamnan** (M'96) was born in Trang, Thailand. He received the B.Eng. degree in telecommunication engineering from the King Mongkut Institute of Technology, Ladkrabang (KMITL), Thailand, in 1992, the M.Sc. degree in communication and signal processing from Imperial College, University of London, London, U.K., in 1995 and the Ph.D. degree in electrical engineering from the University of Surrey, Surrey, U.K., in 2001.

He is currently a Director of the Research Center of Electromagnetic-Wave Applications and Assistant

Professor with the Department of Telecommunication Engineering, Mahanakorn University of Technology, Bangkok, Thailand. His research and teaching interests include RF and microwave passive and active circuits.

Dr. Chongcheawchamnan is a member of the Institution of Electrical Engineers (IEE), U.K.



**Ian D. Robertson** (M'96–SM'05) received the B.Sc. (Eng.) and Ph.D. degrees from King's College London, London, U.K., in 1984 and 1990, respectively.

From 1984 to 1986, he was with the Monolithic Microwave Integrated Circuit (MMIC) Research Group, Plessey Research (Caswell) Ltd. Since then, he has held academic posts with King's College London and the University of Surrey. In June 2004, he became the Centenary Chair in Microwave and Millimeter-Wave Circuits with The University of

Leeds, Leeds, U.K. He is currently an Honorary Editor of the *IEE Proceedings-Microwave, Antennas & Propagation*. He edited *MMIC Design* (IEEE, 1995) and coedited *RFIC and MMIC Design and Technology* (IEE, 2001, 2nd ed.). He has authored or coauthored over papers in the area of microwave integrated circuit (MIC) and MMIC design.

Dr. Robertson has organized numerous colloquia, workshops, and short courses for both the Institution of Electrical Engineers (IEE), U.K., and the IEEE.